Schottky barrier heights at polar metal/semiconductor interfaces

C. Berthod
DPMC, Université de Genève, 24 quai Ernest-Ansermet, CH–1211 Genève 4, Switzerland

N. Binggeli
International Center for Theoretical Physics (ICTP) and INFM DEMOCRITOS National Center, Strada Costiera 11, I–34014 Trieste, Italy

A. Baldereschi
Institut Romand de Recherche Numérique en Physique des Matériaux (IRRMA), CH–1015 Lausanne, Switzerland
(Received 28 February 2003; published 22 August 2003)

Using a first-principle pseudopotential approach, we have investigated the Schottky barrier heights of abrupt Al/Ge, Al/GaAs, Al/AlAs, and Al/ZnSe (100) junctions, and their dependence on the semiconductor chemical composition and surface termination. A model based on linear-response theory is developed, which provides a simple, yet accurate description of the barrier-height variations with the chemical composition of the semiconductor. The larger barrier values found for the anion-terminated surface than for the cation-terminated surface are explained in terms of the screened charge of the polar semiconductor surface and its image charge at the metal surface. Atomic-scale computations show how the classical image charge concept, valid for charges placed at large distances from the metal, extends to distances shorter than the decay length of the metal-induced-gap states.

DOI: 10.1103/PhysRevB.68.085323 PACS number(s): 73.30.+y, 73.40.Ns

I. INTRODUCTION

Metal/semiconductor (MS) interfaces have been the focus of extensive theoretical and experimental studies for several decades.[1–4] To date, however, we are still far from a complete understanding of the factors which control the Schottky barrier height (SBH) at these interfaces. In recent years, new research activities have been developed in the area of band engineering at MS interfaces[5–10] and on the properties of metal/wide-gap-semiconductor contacts.[11–13] These developments have stimulated renewed interest in some basic issues concerning Schottky barriers, and, in particular, in the mechanisms that control the SBH dependence on bulk-semiconductor and interface-specific characteristics.

The problem of Schottky barrier formation has been traditionally addressed by studying the dependence of the SBH on the metal used in the junction.[14] Early studies suggested a Schottky-Mott behavior controlled by the metal work function for highly ionic or wide-gap semiconductors, and a weak dependence on the metal-type and the junction fabrication method for the most covalent semiconductors such as Si or GaAs.[2,14] The latter trend was generally attributed to various Fermi-level pinning mechanisms, such as pinning by metal-induced-gap states (MIGS)[15] at an intrinsic charge neutrality level of the semiconductor[16,17] or pinning by native defect states of the semiconductor at some extrinsic gap level.[18,19] Furthermore, a correlation between Schottky barriers and heterojunction band offsets was observed experimentally for a number of systems,[20] and similarly ascribed to Fermi-level pinning at a bulk reference level. Finally, the effect of the semiconductor ionicity on the SBH trend with the metal work function was examined in pioneering self-consistent studies of jellium/semiconductor contacts, and the trend could also be generally understood in terms of MIGS properties of the semiconductor.[21]

More recent experiments on metal contacts to covalent semiconductors, however, have revealed a much weaker electronic pinning than was previously believed.[2] In particular, there have been reports on considerable changes in metal/Si and metal/GaAs SBH's obtained by altering the structural properties and/or the chemical composition of the interface.[8,22] The conclusion that the SBH does depend most generally on the microscopic atomic structure of the interface has been reached by many authors, both on experimental[2,3,5–8,11,12,22] and theoretical[11,23–28] grounds. While opening a promising line of research on Schottky barrier engineering, these observations complicate seriously the search for simple models of Schottky barrier formation, since the inclusion of the interface atomic structure seems unavoidable.

Given the complexity and variety of the atomic structure at metal/semiconductor contacts, it seems unlikely that a simple unified model could emerge and entirely cover the various facets of Schottky barrier formation. Conversely, a systematic investigation of the problem starting from abrupt, defect free interfaces, and progressively introducing perturbations at the interface could help identifying relevant microscopic mechanisms and provide a firmer basis for modeling Schottky barrier properties. Progress in computational physics has made possible accurate *ab initio* calculations of the electronic structure of MS contacts, and the complexity of the systems which can be examined is steadily increasing; this type of computations can provide the means to carry out such an investigation and probe the correlation between microscopic atomic structures and SBH's. The present study is a step in this direction.

In this paper, we study from first principles the depen-

 ©2003 The American Physical Society

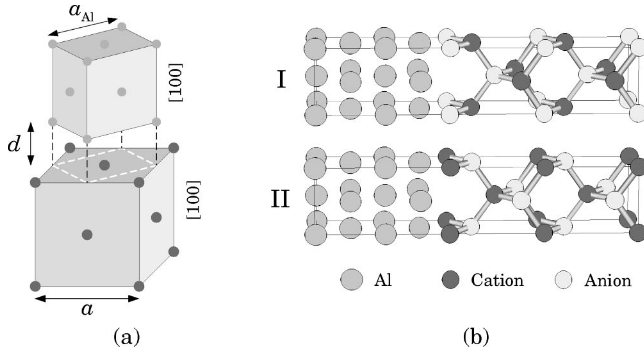

FIG. 1. (a) Epitaxial alignment of Al on the (100) surface of zinc-blende semiconductors verifying the lattice-matching condition $a_{\mathrm{Al}}=a/\sqrt{2}$. (b) Atomic structure of the abrupt Al/semiconductor (100) interface. The semiconductor surface is terminated either by an anion (I) or a cation (II) plane.

dence of the SBH on selected bulk and surface characteristics of the semiconductor, for a given metal. Specifically, we examine abrupt Al/X (100) junctions, where $X=$ (Ge, GaAs, AlAs, and ZnSe) are lattice matched semiconductors of increasing ionicity, and investigate the microscopic mechanisms responsible for the SBH changes with the semiconductor chemical composition and surface termination (cation or anion). A model based on a linear-response-theory scheme is then developed, which explains our *ab initio* results and SBH trends observed experimentally.

II. METHOD OF CALCULATION

We have carried out *ab initio* calculations, within the local-density approximation (LDA) to density-functional theory (DFT), using the pseudopotential method.[29] We used norm-conserving scalar-relativistic Troullier-Martins pseudopotentials[30,31] in the Kleinman-Bylander nonlocal form[32] and the exchange-correlation functional of Ceperley and Alder.[33] The electronic states were expanded on a plane-wave basis set using a kinetic energy cutoff of 20 Ry. We used supercells containing 7 Al layers and 13 semiconductor layers (7+13 supercell) to model defect-free Al/X (100) junctions. In Sec. IV B, we employed larger supercells (7+21) to investigate the screening of substitutional charges placed in the junctions, and to compute the parameters (D_s, δ_s) necessary to model this screening. All supercell calculations were performed with a (2,6,6) Monkhorst-Pack k-point grid.[34]

We considered ideally abrupt epitaxial junctions and neglected atomic relaxation at the interfaces. The effect of atomic relaxation at the Al/GaAs (100) and Al/ZnSe (100) interfaces has been examined in Refs. 11 and 35. Atomic relaxation decreases (increases) the p-type Schottky barriers of the abrupt Al/GaAs (Al/ZnSe) junctions by 0–0.1 eV (Ref. 35) [0.1–0.2 eV (Refs. 11 and 36)], and has no influence on the SBH ordering of the anion- and cation-terminated interfaces.

The epitaxial alignment of Al on the (100) surfaces of the four semiconductors under study is illustrated in Fig. 1(a). This type of alignment corresponds to the lattice-matching condition: $a_{\mathrm{Al}}=a/\sqrt{2}$, where a is the semiconductor lattice parameter. The Al [100] direction is parallel to the semiconductor [100] axis, and the whole Al fcc lattice is rotated by 45° about its [100] axis with respect to the semiconductor substrate. Experimentally—and also in our calculations—Ge, GaAs, AlAs, and ZnSe are lattice-matched semiconductors, and the equilibrium lattice constant of Al is slightly larger (1%) than $a/\sqrt{2}$. This results in a small compressive strain in the Al in-plane lattice parameter, which is accommodated by an elongation (∼3%) of the Al overlayer, assuming pseudomorphic conditions. For the semiconductor lattice parameter, we used the theoretical value $a=5.55$ Å ($a^{\mathrm{expt.}}=5.65$ Å). The metal-semiconductor interlayer distance d at the junction was taken as the average between the (100) interlayer spacings in the semiconductor and in the (strained) Al bulk parts, i.e., $d=1.72$ Å. The polar Al/X (100) junction offers two inequivalent abrupt interfaces, either with anion- or cation-terminated semiconductor surface, which are both considered in our study [see Fig. 1(b)]. In what follows, we will refer to the anion- and to the cation-terminated interface as interface I and II, respectively.

To evaluate the p-type SBH, ϕ_p, we used the same approach as in previous studies:[26,35]

$$\phi_p=\Delta V+\Delta E_p, \tag{1}$$

where ΔV is the electrostatic-potential lineup at the interface and ΔE_p is the difference between the Fermi level in the metal and the valence-band maximum (VBM) in the semiconductor, each measured with respect to the average electrostatic potential in the corresponding crystal. The band-structure term ΔE_p is characteristic of the individual bulk crystals forming the junction. This term was computed using the Kohn-Sham (KS) eigenvalues of standard bulk band-structure calculations. The potential lineup ΔV contains all interface-specific contributions to ϕ_p and was obtained—via Poisson's equation and using a macroscopic average technique[26,35]—from the self-consistent supercell charge density.

For a meaningful comparison of our calculated SBH's with experiment, ΔE_p should include quasiparticle and spin-orbit corrections. The spin-orbit correction is simply $+\Delta_{\mathrm{so}}/3$, where Δ_{so} is the total spin-orbit splitting at the semiconductor valence-band maximum, which was taken from experiment. For a metal, in principle, the *exact* KS Fermi energy and the quasiparticle Fermi energy must coincide at zero temperature.[37] Furthermore, LDA calculations for the work functions of various Al surfaces performed with the same method and the same pseudopotentials as in the present study—and neglecting many-body corrections on the Al Fermi energy—yielded values which agree with the experimental data to within a few tenths of meV.[38] In the present study, therefore, for the metal Fermi energy, we just used the LDA result. The corrected band term is thus $\Delta E_p=\Delta E_p^{\mathrm{KS}}-\Delta E_{\mathrm{qp}}-\Delta_{\mathrm{so}}/3$, where ΔE_p^{KS} is the KS band term and ΔE_{qp} is the difference between the quasiparticle and KS semiconductor VBM energies.

For the quasiparticle corrections, we used the results of GW calculations taken from the literature.[25,39,41] For

TABLE I. Estimated quasiparticle and spin-orbit corrections to ϕ_p^{LDA} for different semiconductors. The calculated Al/X (100) SBH's including these corrections are shown in the last two columns. All numbers are in eV.

Semiconductor X	Estimated correction	ϕ_p I	ϕ_p II
Ge	0.17	0.21	
GaAs	0.25	0.86	0.76
AlAs	0.36	1.45	1.16
ZnSe	0.36	2.18	1.82

Al/GaAs, we used the correction $\Delta E_{\mathrm{qp}}^{\mathrm{GaAs}} = -0.36$ eV evaluated by Charlesworth *et al.*,[25] who employed, for the reference LDA calculations, the same exchange-correlation potential as we do. For Ge (AlAs), we used the correction for GaAs, and the difference between the Ge (AlAs) and GaAs corrections evaluated in Ref. 39, i.e., $\Delta E_{\mathrm{qp}}^{\mathrm{Ge}} - \Delta E_{\mathrm{qp}}^{\mathrm{GaAs}} = +0.09$ eV ($\Delta E_{\mathrm{qp}}^{\mathrm{AlAs}} - \Delta E_{\mathrm{qp}}^{\mathrm{GaAs}} = -0.11$ eV).[40] The quasiparticle corrections to the band structure of ZnSe have been evaluated in Ref. 41. As the LDA band gap in our calculations and in Ref. 41 are different, due to the different pseudopotentials employed, we took the valence-band-edge correction of Ref. 41 and scaled it by the ratio of the difference between the LDA and GW band gap in the two calculations. The resulting estimate for $\Delta E_{\mathrm{qp}}^{\mathrm{ZnSe}}$ is -0.50 eV. Using the experimental spin-orbit splittings $\Delta_{\mathrm{so}}^{X} = 0.30$, 0.34, 0.28, and 0.43 eV for X = Ge, GaAs, AlAs, and ZnSe,[42] the total corrections are 0.17, 0.25, 0.36, and 0.36 eV, respectively.[43] The numerical uncertainty on the absolute value of the SBH's is estimated as ~ 0.1 eV for Al/Ge, Al/GaAs, and Al/AlAs, and as ~ 0.2 eV for Al/ZnSe. For a given interface geometry, however, the relative barrier values ($\Delta\phi_p$ in Table II) are considerably more accurate, i.e, have an estimated numerical accuracy of ~ 50 meV.

III. RESULTS FOR THE SCHOTTKY BARRIER HEIGHTS

The calculated SBH's for the abrupt Al/X (100) interfaces, including many-body and spin-orbit corrections, are given in Table I. We observe a systematic difference between the type-I and type-II interfaces: the p-type SBH is always higher for the type-I (anion-terminated) interface. This difference increases with increasing semiconductor ionicity. Our theoretical results are compared with experimental SBH values in Fig. 2. For the Al/Ge, Al/GaAs, and Al/AlAs systems, the experimental ranges correspond to data obtained by transport measurements. In the case of Al/GaAs, photoemission measurements—performed at low metal coverage—give rise to a wider range of SBH values,[44] but the scattering in the data decreases significantly when thick metallic overlayers are deposited and the barriers are measured by transport techniques. For Al/ZnSe, we are not aware of any transport data and we used photoemission results.

In the case of Al/Ge, no SBH measurement has been performed, to the best of our knowledge, on the (100)-oriented interface. In Fig. 2, we have thus used the existing transport

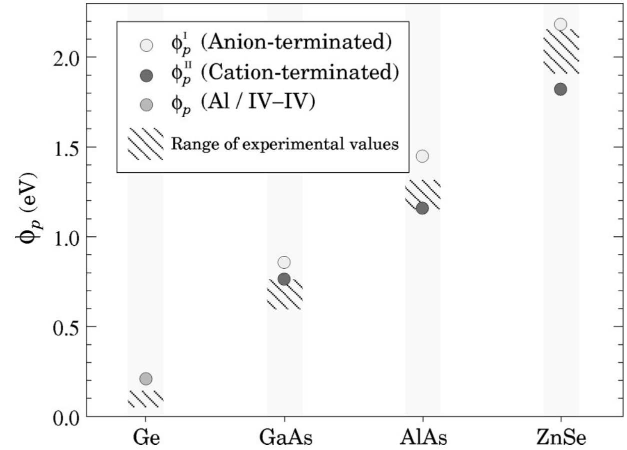

FIG. 2. Schottky barrier heights (SBH's) at Al/X (100) contacts, X = Ge, GaAs, AlAs, and ZnSe. The circles show the calculated SBH's for the ideal anion- and cation-terminated junctions, corrected for quasiparticle and spin-orbit effects. The shaded regions show the ranges of experimental values (see text).

data[45] on Al/n-Ge (111) junctions ($\phi_n = 0.52$–0.61 eV), together with the Ge experimental band gap at room temperature, $E_g^{\mathrm{Ge}} = 0.66$ eV.[46] The resulting barrier heights $\phi_p = 0.05$–0.14 eV compare reasonably well with our calculated value of 0.21 eV. In the case of Al/GaAs (100), the transport measurements give values of ϕ_p between 0.58 eV and 0.76 eV (we used $E_g^{\mathrm{GaAs}} = 1.42$ eV to estimate the p-type barrier heights from measurements performed on Al/n-GaAs junctions).[8–10,47–56] This is in relatively good agreement with our calculated SBH of 0.76 eV for the Ga-terminated interface, and still consistent with our value of 0.86 eV for the As-terminated interface. Concerning the effect of the GaAs-surface stoichiometry on the measured SBH, we note that different conclusions have been reached by different groups. Some studies, including Refs. 48 and 49, have found a small (~ 0.1 eV) difference between the SBH's measured in junctions fabricated on As-rich and on Ga-rich surfaces (As-rich leading to higher ϕ_p, consistent with our results), while other studies, such as Refs. 50 and 53, found no difference.

For the Al/AlAs system, Ref. 49 reports SBH values for Al/n-AlAs (100) ranging from 0.85 to 0.94 eV for various reconstructions of the semiconductor surface, while somewhat higher values, 0.95 and 1.01 eV, have been given in Refs. 55 and 56, respectively. Using the experimental band gap $E_g^{\mathrm{AlAs}} = 2.16$ eV, the resulting range is $\phi_p = 1.15$–1.31 eV, in good agreement with the calculated SBH for the Al-terminated AlAs surface (1.16 eV), and somewhat smaller than the value we find for the As-terminated surface (1.45 eV). The Al/n-ZnSe (100) SBH has been investigated in Refs. 11, 12, and 57 for different reconstructions of the ZnSe (100) surface. Very similar values have been reported for the $c(2\times2)$ and 2×1 reconstructions, namely, $\phi_p = 2.12$–2.15 eV (Refs. 11,12,57) and $\phi_p = 2.11$–2.15 eV,[11,12] respectively, while a lower SBH, $\phi_p = 1.91$ eV, has been measured for the 1×1 reconstruction.[11] These values are in between our values of

1.82 eV for the Zn-terminated and of 2.18 eV for the Se-terminated interface.

The general agreement between theory and experiment in Fig. 2 indicates that our calculations for ideal MS structures (abrupt interfaces with no atomic relaxation) capture the general trend of the SBH with the chemical composition of the semiconductor. We note that for Al/ZnSe, the inclusion of the appropriate reconstruction and relaxation brings the theoretical results in very close agreement with the experimental values.[11]

IV. INTERPRETATION AND MODELS

A. General trend with the semiconductor chemical composition

Experimentally, a correlation was found between Schottky barriers and heterojunction band offsets.[20] A large number of MS contacts and semiconductor heterojunctions were shown to verify, within 0.4 eV, the transitivity relationship:

$$\phi_p[M/S_1]-\phi_p[M/S_2]=\Delta E_{\mathrm{VBO}}[S_1/S_2], \qquad (2)$$

where M is a metal (such as Al or Au; in general, neither a highly reactive nor a transition metal[58]), S_1 and S_2 are two semiconductors, and $\Delta E_{\mathrm{VBO}}[S_1/S_2]$ is the corresponding valence-band offset (VBO). This correlation was most often observed for MS junctions used in transport measurements, i.e., which had been annealed for fabrication of the contacts. The experimental data in Fig. 2 are in general agreement with the above empirical transitivity rule.

We note that the transitivity rule, as formulated in Eq. (2), disregards any dependence of the SBH on the microscopic interface structure, and cannot therefore give a complete account of the theoretical results in Fig. 2. Also, recent theoretical and experimental studies have shown that the band offset at heterovalent semiconductor heterojunctions depends critically on the orientation and other microscopic details of the interface.[59–61] The right-hand side of Eq. (2) is thus ill defined, in general, for heterovalent semiconductors.

In this section, we concentrate on the average SBH $\bar{\phi}_p=\frac{1}{2}(\phi_p^{\mathrm{I}}+\phi_p^{\mathrm{II}})$ of the abrupt, defect-free type-I and type-II interfaces, and propose a model for its variation with the semiconductor chemical composition, derived from an atomic-scale approach. We show that this variation is controlled essentially by the same bulk mechanism that determines band offsets at nonpolar, defect-free semiconductor heterojunctions.[59] The splitting $\Delta\phi_p=\phi_p^{\mathrm{I}}-\phi_p^{\mathrm{II}}$ due to the semiconductor-surface termination will be the focus of the following section.

Similar to the SBH, the VBO may be written as $\Delta E_{\mathrm{VBO}}=\Delta E_v+\Delta V$, where ΔE_v is the difference between the VBM energies of the two semiconductors, each measured relative to the mean electrostatic potential in the corresponding crystal, and ΔV is the electrostatic potential lineup at the interface. Since the band-structure terms ΔE_v and ΔE_p [in Eq. (1)] are differences between bulk values of the individual crystals forming the junction, they verify by definition the transitivity relationship in Eq. (2). All nontransitive contributions are contained thus in the potential lineup terms ΔV.

In the case of semiconductor heterojunctions, a linear-response-theory (LRT) approach, which focuses on ΔV and treats the interface as a perturbation with respect to a bulk reference system, has provided an accurate general description of band-offset trends.[59,60] Based on this approach and comparison with fully self-consistent *ab initio* calculations, it has been shown, in particular, that in the case of defect-free, isovalent lattice-matched semiconductor heterojunctions, ΔV is determined by the properties of the bulk constituents (as opposed to interface-specific features such as interface orientation or interface abruptness). Specifically, if S_1 and S_2 are the two semiconductors, with anion (cation) species a_1 (c_1) in S_1 and a_2 (c_2) in S_2, the potential lineup is given within LRT by:[59]

$$\Delta V[S_1/S_2]=\frac{2\pi e^2}{3\Omega}\int r^2[\Delta n_a(\boldsymbol{r})+\Delta n_c(\boldsymbol{r})]d\boldsymbol{r}, \qquad (3)$$

where the integration is over the whole space, Ω is the volume of the bulk unit cell, and Δn_a (Δn_c) is the electronic charge density induced by a single anion (cation) substitution $a_1\rightarrow a_2$ ($c_1\rightarrow c_2$) in the bulk semiconductor S_1.[62] Based on this LRT approach, it has also been shown that in the case of heterovalent lattice-matched semiconductors, Eq. (3) also applies in the specific case of defect-free interfaces with the nonpolar (110) orientation.[60]

Using a similar linear-response scheme for ΔV, we show in the Appendix that the average SBH $\bar{\phi}_p$ can be described by the following model:

$$\bar{\phi}_p^{\mathrm{mod}}=\phi_p[\mathrm{Al}/\langle X\rangle\ \ (100)]+\Delta E_{\mathrm{VBO}}[\langle X\rangle/X\ \ (110)]. \qquad (4)$$

The first term on the right-hand side of Eq. (4) is the SBH at the (100) interface between Al and the group-IV virtual crystal, denoted by $\langle X\rangle$, which is obtained by averaging the anion and cation pseudopotentials of the III-V or II-VI compound X ($X=$ GaAs, AlAs, ZnSe). The second term is the VBO of the nonpolar $\langle X\rangle/X$ (110) heterojunction.

The basic approximation to derive Eq. (4) is to construct the charge densities of the Al/X I and II junctions (and hence their average lineup) starting from the reference Al/$\langle X\rangle$ system, by adding a linear superposition of the charge densities induced in the virtual crystal $\langle X\rangle$ by single anion and cation substitutions that transform $\langle X\rangle$ into X. The Al/$\langle X\rangle$ (100) junction is an optimal reference system in this context, which minimizes the deviations of $\bar{\phi}_p$ from $\bar{\phi}_p^{\mathrm{mod}}$ in Eq. (4); these deviations vanish to the first order in the ionic substitutions which transform Al/$\langle X\rangle$ into the Al/X I and II junctions.

It is also possible to use as a reference system another Al/group-IV (100) junction, whose density is sufficiently close to the average density of the Al/X I and II junctions. For instance, one may use Al/Ge as a common reference system and obtain (see the Appendix):

$$\bar{\phi}_p^{\mathrm{mod}'}=\phi_p[\mathrm{Al/Ge}\ \ (100)]+\Delta E_{\mathrm{VBO}}[\mathrm{Ge}/X\ \ (110)]. \qquad (5)$$

The deviations of $\bar{\phi}_p$ from $\bar{\phi}_p^{\mathrm{mod}'}$ in Eq. (5) include, in this case, a first-order correction in the substitutions. The latter correction can be identified with the dipole induced in the

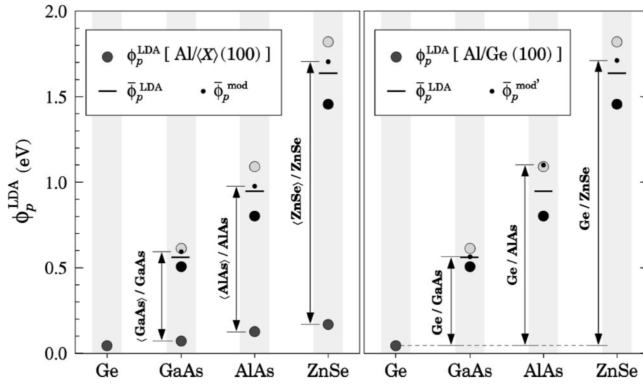

FIG. 3. Comparison of the average SBH $\bar{\phi}_p^{\rm LDA}$ at the Al/X (100) I and II interfaces with the model predictions, Eq. (4) (left panel) [Eq. (5) (right panel)]. The horizontal bar shows the average SBH and the small dot indicates the model result, i.e., the sum of the SBH at the Al/⟨X⟩ (100) [Al/Ge (100)] junction (gray circles [dashed line]) and the VBO at the ⟨X⟩/X (110) [Ge/X (110)] interface (double arrows). The quasiparticle and spin-orbit corrections are not included; these contributions trivially verify the transitivity relationship in Eq. (2).

reference Al/Ge (100) junction by isovalent Ge →⟨X⟩ substitutions performed within the first one to three Ge atomic layers closest to the interface (see the Appendix); such a dipolar term is generally small for isovalent substitutions (∼0.1 eV or less, see Ref. 28), and will be neglected here.

In Fig. 3, we compare graphically the model predictions, Eqs. (4) and (5), with the calculated average SBH of the Al/X I and II interfaces. The (110) VBO's have been computed using supercells containing eight planes of each semiconductor in the ideal (unrelaxed) lattice-matched geometry. The same energy cutoffs and k-points grids have been used as in the calculations of the Schottky barriers. The SBH's of the Al/⟨X⟩ (100) junctions have been obtained using the same parameters as for the Al/X (100) I and II interfaces. The results in Fig. 3 show that Eqs. (4) and (5) provide a fairly accurate (±0.15 eV) description of the average SBH $\bar{\phi}_p$. We note that the SBH's at the Al/⟨X⟩ junctions are all small, due to the small band gaps of the virtual crystals (<0.4 eV), and similar to the LDA SBH at the Al/Ge (100) interface (0.04 eV). The results in Fig. 3 show that the (110) VBO— a bulk-related quantity in our calculations—controls the general increase of the barriers from the group-IV to the III-V and to the II-VI semiconductors.

B. Effect of surface termination

We will show here that the difference $\Delta\phi_p = \phi_p^{\rm I} - \phi_p^{\rm II}$ due to the semiconductor-surface termination in Fig. 2—and in particular the fact that the SBH is systematically higher for the anion than for the cation termination—can be understood in terms of surface-charge and image-charge effects. The mechanism is illustrated in Fig. 4.

With respect to the Al/⟨X⟩ interface, the ionic charge distributions of the interfaces I and II are obtained by substituting an anion (charge $+\bar{\sigma}$) on each anionic site and a cation (charge $-\bar{\sigma}$) on each cationic site, as indicated in Fig. 4(a).

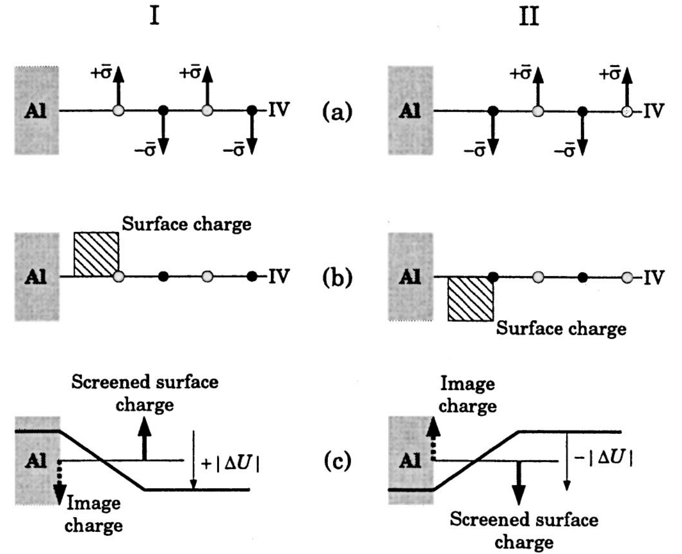

FIG. 4. (a) Planar average of the difference between the ionic charge densities of the anion- (cation-) terminated Al/X (100) interface and the Al/⟨X⟩ (100) interface; $\bar{\sigma}=1$ for the semiconductors $X=$ GaAs, AlAs, and $\bar{\sigma}=2$ for $X=$ ZnSe. (b) Macroscopic average of the ionic charge density difference. (c) Positive (negative) potential difference established at the interface I (II) by a positive (negative) surface charge and its image charge at the metal surface.

For the III-V and II-VI compounds, we have $\bar{\sigma}=1$ and $\bar{\sigma}=2$, respectively, in units of charge per unit-cell surface in the (100) plane. The arrows in Fig. 4(a) represent opposite δ functions on each anionic and cationic (100) plane, corresponding to the planar average of the ionic point-charge density. The macroscopic average[59,60] of this ionic charge distribution is represented in Fig. 4(b). In the bulk semiconductor, the macroscopic average eliminates the atomic-scale oscillations of the planar charge density; at the interface, however, a positive (negative) charge density subsists in the junction I (II). This macroscopic charge has a density $\rho = \pm 2\bar{\sigma}/a$ and extends over a distance $a/4$ between the last Al plane and the first semiconductor plane. It is therefore equivalent to a surface charge of density $\sigma = \pm\bar{\sigma}/2$.

Within a classical macroscopic description, a plane of charge in a semiconductor is screened by the dielectric constant ϵ_∞ of the host material. Furthermore, in the presence of a metal, the screened surface charge is neutralized by an image charge induced at the metal surface, and a potential difference is thus established between the two charges [see Fig. 4(c)]. If σ is the density of surface charge in the semiconductor, x is the position of the plane of surface charge, and x_i is the position of the metal surface or image charge, the potential difference obtained from classical electrostatics is

$$\Delta U(x,\sigma) = 4\pi e^2 \frac{\sigma}{\epsilon_\infty}(x - x_i). \tag{6}$$

As can be seen from Fig. 4(c), in the junction I, such a dipole lowers the average potential energy in the semiconductor with respect to its value in the metal, increasing the SBH

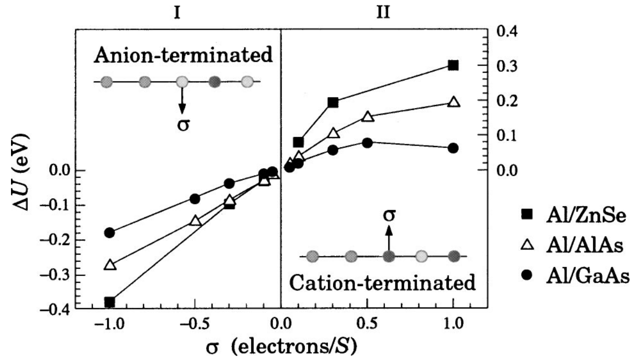

FIG. 5. Schottky barrier modification ΔU induced by a bare surface charge σ per unit-cell surface $S=a^2/2$ on the first semiconductor layer closest to the metal in the Al/X (100) I and II junctions (see insets; the same symbols for the atomic layers are used as in Fig. 1).

ϕ_p; conversely, in the junction II, the dipole raises the average potential in the semiconductor, decreasing ϕ_p. The mechanism illustrated in Fig. 4 thus provides a qualitative explanation for the difference between the SBH's of the interfaces I and II. Of course, the classical limit given by Eq. (6) is expected to be correct only for a charge placed at a large distance from the metal. As we will see below, however, closer to the metal, the above type of description may still be used provided the inhomogeneous nature of the screening near the metal is taken into account.

To check that the mechanism in Fig. 4 can indeed account for the SBH differences $\Delta\phi_p$, we have calculated the changes in the lineup (and hence in the SBH) induced by surface charges of varying magnitude, placed on the semiconductor plane closest to the metal in the Al/X I and II junctions. At the interface I (II), a surface charge of density $-|\sigma|$ $(+|\sigma|)$ was introduced by replacing the anion A (cation C) of the semiconductor layer adjacent to the metal surface by a virtual ion $\langle A_{1-\sigma/2}C_{\sigma/2}\rangle$ $(\langle C_{1-\sigma/2}A_{\sigma/2}\rangle)$. The resulting changes ΔU in the SBH obtained from the *ab initio* calculations are shown in Fig. 5. The negative (positive) surface charge decreases (increases) the p-type SBH of the anion-terminated (cation-terminated) interfaces, consistent with the screened surface-charge and image-charge description in Fig. 4(c). We also note that, consistent with the latter description, the bare monopole is replaced by an interface dipole in the multipole expansion of the total (electronic plus ionic) charge disturbance.

The macroscopic average of the difference between the ionic potentials in the junctions II and I, in Fig. 4(a), is equivalent to a surface charge $\sigma=-1$ at the interface for the III-V semiconductors and $\sigma=-2$ for the II-VI semiconductors. Therefore, focusing on the effect of the macroscopic charges only and to the first order in the perturbation, the modification of the SBH in the junctions I for $\sigma=-1$ (-2) should be equal to the difference $\phi_p^{\mathrm{II}}-\phi_p^{\mathrm{I}}$ for the III-V (II-VI) semiconductors. Similarly, the change of the SBH in the junctions II induced by a surface charge $\sigma=+1$ $(+2)$ should be equal to $\phi_p^{\mathrm{I}}-\phi_p^{\mathrm{II}}$. Our *ab initio* results in Fig. 5 show, however, that the responses ΔU of the two interfaces are not linear when $|\sigma|\gtrsim 0.5$ and differ in magnitude. Therefore, we take the average $\overline{\Delta U}$ between the potential differences induced in the junctions I and II as our estimate for the difference $\Delta\phi_p$. The results are shown in Table II. For Al/ZnSe, we reported the calculated SBH changes for $\sigma=\pm 2$ (not shown in Fig. 5). The average values $\overline{\Delta U}$ are seen to describe well the calculated difference $\Delta\phi_p$ and also the increase of $\Delta\phi_p$ when the semiconductor ionicity increases.

TABLE II. Comparison of the average SBH change $\overline{\Delta U}$ induced by surface charges $\sigma=\pm 1$ (GaAs, AlAs) and $\sigma=\pm 2$ (ZnSe) at the interface, with the difference $\Delta\phi_p=\phi_p^{\mathrm{I}}-\phi_p^{\mathrm{II}}$ between the SBH of the anion- and cation-terminated Al/X (100) junctions (see text). The last column shows the results of the model (11). All energies are in eV.

X	$\Delta\phi_p$	$\lvert\Delta U\rvert$		$\overline{\Delta U}$	D_s	δ_s	$\Delta\phi_p^{\mathrm{mod}}$
		I	II		(eV^{-1} Å^{-2})	(Å)	Eq. (11)
GaAs	0.10	0.18	0.06	0.12	0.051	2.5	0.10
AlAs	0.29	0.27	0.19	0.23	0.060	2.0	0.13
ZnSe	0.36	0.68	0.24	0.46	0.041	1.8	0.40

Although this supports the surface-charge and image-charge picture in Fig. 4(c), Eq. (6) needs to be revisited for charges placed close to the metal surface. For example, in the case of a test charge $\sigma=0.1$ on the first semiconductor layer, we obtain from Eq. (6) a potential difference $\Delta U=82$ meV, using for the distance $x-x_i$ the value $d/2$, where $d=1.72$ Å is the interplanar distance at the interface (see Fig. 1), and for ϵ_∞ the theoretical dielectric constant of GaAs, $\epsilon_\infty^{\mathrm{GaAs}}=12.4$.[26] This result is more than five times larger than the *ab initio* result for the potential difference obtained for Al/GaAs and shown in Fig. 5.

In Ref. 26, we observed a somewhat similar behavior in the case of local dipoles inserted in the Al/GaAs (100) junction. In the latter case, *ab initio* calculations were performed to determine the change in the lineup Δu induced by a dipole layer (i.e., two test charges $+\sigma$ and $-\sigma$ placed on two adjacent cation-anion planes) introduced at various distances x from the metal, within the semiconductor. In this numerical experiment, the bare dipole perturbation is $\Delta u_b=4\pi e^2\sigma l$, where l is the separation between the charged planes, and from the computed Δu, we could directly measure the effective dipole screening $\epsilon_{\mathrm{eff}}^{\mathrm{dip}}=\Delta u_b/\Delta u$ as a function of the dipole position x in the junction. This screening was found to be strongly inhomogeneous and to increase exponentially as the dipole was approaching the metal surface. This was attributed to the MIGS tails and their high polarizability in the interface region. We also proposed a model for $\epsilon_{\mathrm{eff}}^{\mathrm{dip}}$ which proved very accurate to describe the SBH changes $\Delta u(x,\sigma)$ in the linear-response regime (i.e., to the first order in σ):[26]

$$\epsilon_{\mathrm{eff}}^{\mathrm{dip}}(x)\approx\epsilon_\infty+4\pi e^2 D_s(E_{\mathrm{F}},x)\,\delta_s. \tag{7}$$

Here, $D_s(E_{\mathrm{F}},x)$ is the MIGS surface density of states at the Fermi energy and at the position x of the dipole, and δ_s is the decay length of the MIGS. The model (7) is also consistent with earlier MIGS-based model descriptions of Schottky barrier properties.[21,23,63]

In order to predict, in general, the effect of the surface termination in MS junctions, we would like to develop a model for ΔU that takes into account the inhomogeneous nature of the electronic screening in the MIGS region and that is consistent with our previous results on the effect of the dipole layers on the SBH. In particular, this model should be consistent with the fact that, in the linear-response regime (small $|\sigma|$), the sum of the SBH modifications induced separately by two charges $+\sigma$ and $-\sigma$ separated by a small distance l, $\Delta U(x-l/2,\sigma)$ and $-\Delta U(x+l/2,\sigma)$, respectively, must be equal to the SBH modification induced by the corresponding dipole:

$$\Delta U(x-l/2,\sigma)-\Delta U(x+l/2,\sigma)=-\frac{4\pi e^2\sigma l}{\epsilon_{\mathrm{eff}}^{\mathrm{dip}}(x)}. \quad (8)$$

Expanding the left-hand side of Eq. (8) to the first order in l, we obtain the differential equation

$$\frac{\partial\Delta U}{\partial x}(x,\sigma)=\frac{4\pi e^2\sigma}{\epsilon_{\mathrm{eff}}^{\mathrm{dip}}(x)}. \quad (9)$$

With our expression for $\epsilon_{\mathrm{eff}}^{\mathrm{dip}}(x)$ in Eq. (7) and a surface density of states that decays exponentially,[64] $D_s(E_{\mathrm{F}},x)=D_s(E_{\mathrm{F}},0)\exp(-x/\delta_s)$, the solution of Eq. (9) with the boundary condition $\Delta U(x_0)=0$ is

$$\Delta U(x,\sigma)=4\pi e^2\frac{\sigma}{\epsilon_\infty}\left[x-x_0-\delta_s\ln\frac{\epsilon_{\mathrm{eff}}^{\mathrm{dip}}(x_0)}{\epsilon_{\mathrm{eff}}^{\mathrm{dip}}(x)}\right], \quad (10)$$

where x is the position of the surface charge. We note that for large values of x, we recover the classical limit given by Eq. (6), with $x_i=x_0+\delta_s\ln[\epsilon_{\mathrm{eff}}^{\mathrm{dip}}(x_0)/\epsilon_\infty]$.

With the exception of x_0, all parameters necessary to evaluate $\Delta U(x,\sigma)$ in Eq. (10) can be obtained straightforwardly from *ab initio* calculations performed either for the bulk semiconductor (ϵ_∞) or for the unperturbed Al/X junction (the MIGS-related parameters). In Table II, we have reported our calculated values for the MIGS parameters $D_s\equiv D_s(E_{\mathrm{F}},0)$ and δ_s. These quantities were obtained from the calculated macroscopic average of the local density of states, $N(E,x)$, as $D_s=\int_0^\infty N(E_{\mathrm{F}},x)\,dx$ and $\delta_s=(1/D_s)\int_0^\infty x\,N(E_{\mathrm{F}},x)\,dx$, where the origin ($x=0$) was taken as the midpoint between the last Al and the first semiconductor plane, and ∞ indicates a position well inside the semiconductor (the center of the semiconductor slab in the supercell) where the MIGS vanish. As the values of D_s and δ_s are slightly different for the interfaces I and II, we reported in Table II the average between the values calculated for the two interfaces.[65]

In order to obtain an estimate for x_0, and also to test the model in Eq. (10), we have investigated *ab initio* the spatial dependence of ΔU in the linear-response regime by introducing a small test surface charge $\sigma=\pm0.05$ in the As-terminated Al/GaAs junction at different distances from the interface. This was done by replacing single layers of As (Ga) ions by virtual $\langle As_{0.95}Si_{0.05}\rangle$ ($\langle Ga_{0.95}Si_{0.05}\rangle$) anions (cations). As an example, we show in Fig. 6, the *ab initio* results for the charge density and potential induced by such a test charge on the sixth semiconductor layer from the metal. The macroscopic averages of the ionic, electronic, and total charge densities are displayed in Fig. 6(a). We have used a Gaussian filter function with full width at half maximum $a/2$ for the macroscopic average. This allows one, in particular, to distinguish the image-charge contribution to the total charge density, close to the Al surface. The macroscopic average of the induced total electrostatic potential is displayed in Fig. 6(b). The corresponding potential difference is $\Delta U=0.24$ eV.

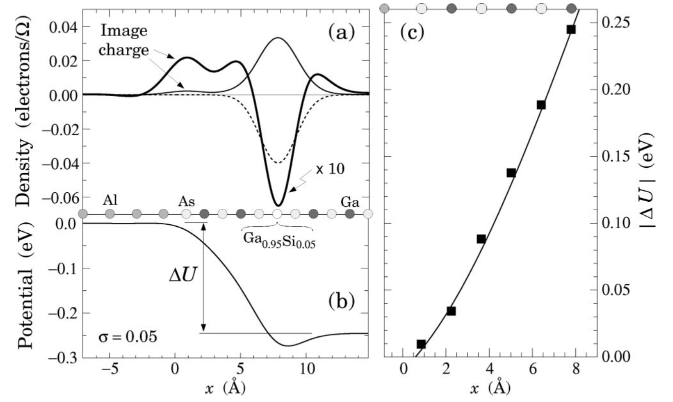

FIG. 6. (a) Macroscopic average of the electronic (thin solid line) and ionic (dotted line) charge densities induced by a plane of $\langle Ga_{0.95}Si_{0.05}\rangle$ virtual ions in the As-terminated Al/GaAs (100) junction. A Gaussian filter function was used for the macroscopic average. The thick solid line is the sum of the electronic and ionic densities, scaled by a factor of 10. (b) Macroscopic average of the corresponding induced total electrostatic potential. The resulting potential difference ΔU is also indicated. (c) Schottky barrier modification $|\Delta U|$ (filled squares) obtained for a surface charge $|\sigma|=0.05$ as a function of its position within the semiconductor, in the As-terminated Al/GaAs junction. The symbols give the results of the self-consistent calculations. The solid line corresponds to the prediction of Eq. (10) with $x_0=0.6$ Å. The atomic positions are indicated using the same symbols for the atoms as in Fig. 1. The calculations were done in a $7+21$ supercell.

In Fig. 6(c), we have plotted the discontinuity $|\Delta U|$ induced by the test charge as a function of its position in the Al/GaAs junction. With the theoretical dielectric constant of GaAs ($\epsilon_\infty^{\mathrm{GaAs}}=12.4$) and the calculated values of D_s and δ_s given in Table II, the best fit of Eq. (10) to the data in Fig. 6(c) is obtained with $x_0=0.6$ Å. The model results obtained from Eq. (10) using $x_0=0.6$ Å have been reported in Fig. 6(c), and compare well with the results of the self-consistent calculations as a function of the distance.

Having a reasonable estimate for x_0, we may now use Eq. (10) to obtain also an estimate for the difference between the SBH's of the interfaces I and II. As we have seen before, this difference may be evaluated as the potential change induced, to the first order, by a surface charge $\bar{\sigma}=1$ (2) per unit-cell surface on the first plane of the III-V (II-VI) semiconductor, i.e., at a position $x=d/2$ with $d=1.72$ Å (see Fig. 1). The resulting estimate $\Delta\phi_p^{\mathrm{mod}}$ for the difference $\Delta\phi_p$ is thus

$$\Delta\phi_p^{\mathrm{mod}}=4\pi e^2\frac{\bar{\sigma}}{\epsilon_\infty}\left[d/2-x_0-\delta_s\ln\frac{\epsilon_{\mathrm{eff}}^{\mathrm{dip}}(x_0)}{\epsilon_{\mathrm{eff}}^{\mathrm{dip}}(d/2)}\right]. \quad (11)$$

The results obtained with this model are displayed in Table II. To evaluate $\Delta\phi_p^{\mathrm{mod}}$, we have used the theoretical value of the semiconductor dielectric constant ϵ_∞^X ($X=$GaAs, AlAs, and ZnSe),[66] the calculated values of the surface density of states D_s and MIGS decay length δ_s given in Table II for the Al/GaAs, Al/AlAs, and Al/ZnSe junctions, and $x_0=0.6$ Å for all systems. The model results, in Table II, yield the correct trend and order of magnitude for the difference between the SBH's. We note that decreasing x_0 increases $\Delta\phi_p^{\mathrm{mod}}$, but does not affect the trend. The same conclusion applies when a possible change in x_0, from GaAs to AlAs and to ZnSe, is taken into account by scaling the x_0 value obtained for GaAs with the ratio of the MIGS decay length, i.e., $\delta_s^X/\delta_s^{\mathrm{GaAs}}$.[67]

Although the present model approach provides a consistent picture of the effect of selected perturbations at MS interfaces, we would like to caution the reader that our model description applies to unrelaxed interfaces. In this connection, it should be pointed out that a LRT model (based on dynamical effective charges) is available in the literature for quantitative predictions of the atomic relaxation contribution to the SBH.[27]

V. CONCLUSION

Using a first-principle pseudopotential approach, we have investigated the Schottky barrier heights of abrupt lattice-matched Al/Ge, Al/GaAs, Al/AlAs, and Al/ZnSe (100) junctions, and their dependence on the semiconductor chemical composition and surface termination. The sensitivity of the SBH to microscopic interface features reveals the limits of the currently accepted semiempirical models of Schottky barriers. Such model theories generally neglect the effects of the microscopic interfacial morphology. This is due in part to the complexity of the actual atomic structure of most MS contacts, and also to the relatively limited information available on the atomic-scale geometry of buried interfaces.

Based on our *ab initio* studies, we have derived models which explicitly include the effects of the interface atomic structure in the case of some prototype defect-free, lattice-matched geometries. These models retain, within specific ranges of applicability, the same accuracy as the *ab initio* calculations. They show, in particular, that while the variation of the average SBH of the abrupt, anion- and cation-terminated Al/semiconductor (100) interfaces can be explained mainly in terms of the bulk properties of the semiconductors, the difference between the barrier heights of the anion- and cation-terminated interfaces results from a microscopic dipole generated by the screened charge of the polar semiconductor surface and its image charge at the metal surface. Our atomic-scale computations have also allowed us to show how the classical image-charge concept, valid for charges placed at large distances from the metal, can be extended to distances shorter than the decay length of the metal-induced-gap states.

ACKNOWLEDGMENTS

One of us (C.B.) acknowledges support by the Swiss National Science Foundation under Grant No. 20-47065.96. The computations were performed at the CSCS in Manno.

APPENDIX: MODEL FOR THE AVERAGE SBH OF THE ANION- AND CATION-TERMINATED INTERFACES

In order to explain the behavior of the average SBH $\bar{\phi}_p$ with the semiconductor composition, we have extended to MS contacts a linear-response-theory approach commonly used to study band offsets at semiconductor heterojunctions.[59,60] The present analysis is also an extension to *heterovalent* semiconductors of an approach outlined in Ref. 28 to model the Schottky-barrier changes with the alloy composition in Al/$\mathrm{Ga}_{1-x}\mathrm{Al}_x$As junctions.

We are interested in the average potential lineup $\overline{\Delta V}=\frac{1}{2}(\Delta V^{\mathrm{I}}+\Delta V^{\mathrm{II}})$, where $\Delta V^{\mathrm{I(II)}}$ is the potential lineup at the interface I (II), for which we want to establish the following model:

$$\overline{\Delta V}\approx\Delta V[\mathrm{Al}/\langle Y\rangle\ \ (100)]+\Delta V[\langle Y\rangle/X\ \ (110)]. \quad (A1)$$

The first term on the right-hand side of Eq. (A1) is the potential lineup at the reference (100) junction between Al and a group-IV (real or virtual) crystal $\langle Y\rangle$ (e.g., the virtual crystal $\langle X\rangle$ or Ge), having a charge density close to the average charge density of the Al/X I and II junctions. The second term is the lineup at the nonpolar (110) interface between the group-IV crystal $\langle Y\rangle$ and the semiconductor X. To derive Eq. (A1), we write the self-consistent electrostatic potential at the Al/X (100) I (II) junction as

$$V^{\mathrm{I(II)}}(\boldsymbol{r})=V_0(\boldsymbol{r})+V_1^{\mathrm{I(II)}}(\boldsymbol{r}), \quad (A2)$$

where $V_0(\boldsymbol{r})$ is the electrostatic potential at the Al/$\langle Y\rangle$ (100) junction. The average lineup $\overline{\Delta V}$ can be expressed, according to Eq. (A2), as $\overline{\Delta V}=\Delta V_0+\Delta V_1$, where $\Delta V_0\equiv\Delta V[\mathrm{Al}/\langle Y\rangle\ (100)]$ and ΔV_1 is the lineup of the potential

$$V_1(\boldsymbol{r})=\frac{1}{2}[V_1^{\mathrm{I}}(\boldsymbol{r})+V_1^{\mathrm{II}}(\boldsymbol{r})]. \quad (A3)$$

The potential $V_1^{\mathrm{I(II)}}$ is the self-consistent electrostatic potential induced in the Al/$\langle Y\rangle$ (100) junction by the ionic substitutions, $\langle Y\rangle\rightarrow$anion and $\langle Y\rangle\rightarrow$cation, performed in the semiconductor, which transform the Al/$\langle Y\rangle$ system into the type-I (type-II) Al/X system. Thus, V_1^{I} and V_1^{II} have long-range contributions associated with each heterovalent anion and cation substitution in the group-IV crystal. These long-range terms cancel out in the average in Eq. (A3), since each anion (cation) substitution in V_1^{I} is compensated by a cation (anion) substitution associated with the *same site* in V_1^{II}. The average potential V_1 has therefore a well-defined macroscopic average in the semiconductor, which is equal to ΔV_1, since $V_1(\boldsymbol{r})$ vanishes in the metal.

One may thus evaluate ΔV_1 using a perturbative approach neglecting intersite interactions in the ionic substitutions, because of the short-ranged nature of the potentials associated

TABLE III. Comparison of the average potential lineup $\overline{\Delta V}$ at the Al/X (100) I and II interfaces with the predictions of the model, $\overline{\Delta V} \approx \Delta V[\mathrm{Al}/\langle Y\rangle\ (100)] + \Delta V[\langle Y\rangle/X\ (110)]$ [Eq. (A1)], using $\langle Y\rangle = \langle X\rangle$ ($\overline{\Delta V}^{\mathrm{mod}}$) and $\langle Y\rangle = \mathrm{Ge}$ ($\overline{\Delta V}^{\mathrm{mod}'}$). All numbers are in eV.

X	$\overline{\Delta V}$	ΔV		$\overline{\Delta V}^{\mathrm{mod}}$	ΔV		$\overline{\Delta V}^{\mathrm{mod}'}$
		Al/$\langle X\rangle$ (100)	$\langle X\rangle$/X (110)		Al/Ge (100)	Ge/X (110)	
GaAs	−2.34	−2.18	−0.12	−2.30	−2.05	−0.28	−2.33
AlAs	−2.01	−1.97	−0.01	−1.98	−2.05	+0.20	−1.85
ZnSe	−3.30	−2.85	−0.38	−3.23	−2.05	−1.17	−3.22

with each individual site. Within this approximation, V_1 is given by (i) the superposition of the potentials induced by *isolated* anion and cation substitutions in the bulk crystal $\langle Y\rangle$ plus (ii) a correction due to the deviations from the bulk response for substitutions performed near the MS interface.

By construction, the potential lineup obtained from (i) is orientation independent and equal to the potential lineup $\Delta V'[\langle Y\rangle/X\ (110)]$ at the nonpolar $\langle Y\rangle/X$ (110) interface, built from a superposition of the same isolated charge-density responses on one side of the X (110) homojunction. Furthermore, previous *ab initio* and LRT studies of semiconductor heterojunctions have shown that the deviation of the lineup ΔV (110) from the transitivity rule, and hence from $\Delta V'$ (110), is typically less than 0.1 eV in IV-IV/III-V junctions, and of the order of 0.1 eV in IV-IV/II-VI junctions.[59,60] We may therefore replace $\Delta V'[\langle Y\rangle/X\ (110)]$ with $\Delta V[\langle Y\rangle/X\ (110)]$ to obtain the contribution from (i) to ΔV_1.

The correction to the lineup induced by (ii) is given, to the first order in the substitutions, by $\Delta V_{\mathrm{corr.}} = \Sigma_i d_i$, where $d_i = 4\pi e^2 \int dx\, x \Delta n_i(x)$ is the dipole and $n_i(x)$ is the charge density, induced by the $\langle Y\rangle \rightarrow$anion or $\langle Y\rangle \rightarrow$cation layer substitution within the ith atomic plane from the interface in the Al/$\langle Y\rangle$ junction. In practice, the dipoles d_i vanish beyond the third to fourth atomic plane from the junction, and $\Delta V_{\mathrm{corr.}}$ is generally of the order of 0.1 eV for isovalent substitutions.[28] Furthermore, when the Al/$\langle X\rangle$ junction is used as a reference system, $\Delta V_{\mathrm{corr.}}$ exactly vanishes, because the corrections are opposite in the I and II junctions and cancel out in the average leading to ΔV_1. The correction $\Delta V_{\mathrm{corr.}}$ is therefore bound to be small ($\sim$0.1 eV) when the reference system is an Al/$\langle Y\rangle$ (100) junction with a density close to the average density of the Al/X I and II junctions. We will thus neglect this correction, which leads to $\Delta V_1 \approx \Delta V[\langle Y\rangle/X(110)]$, and hence to Eq. (A1).

In Table III, the average potential lineup at the Al/X (100) I and II interfaces is compared to the predictions of the model, Eq. (A1), obtained with $\langle Y\rangle = \langle X\rangle$ and $\langle Y\rangle = \mathrm{Ge}$. The agreement between $\overline{\Delta V}^{\mathrm{mod}}$ [$\overline{\Delta V}^{\mathrm{mod}'}$] and the calculated $\overline{\Delta V}$ is quite good, the discrepancy being 2% [8%] or less when the Al/$\langle X\rangle$ (100) [Al/Ge (100)] junction is used as a reference system. Introducing the band energies in Eq. (A1), we obtain Eq. (4) [Eq. (5)] with $\langle Y\rangle = \langle X\rangle$ [$\langle Y\rangle = \mathrm{Ge}$].

[1] E. H. Rhoderick and R. H. Williams, *Metal-Semiconductor Contacts* (Clarendon, Oxford, 1988).

[2] L. J. Brillson, in *Handbook on Semiconductors*, edited by P. T. Landsberg (North Holland, Amsterdam, 1992), Vol. 1, p. 281.

[3] R. T. Tung, in *Materials Interfaces, Atomic-Level Structures and Properties*, edited by D. Wolf and S. Yip (Chapman & Hall, London, 1992), p. 550.

[4] G. Margaritondo, Rep. Prog. Phys. **62**, 765 (1999).

[5] S. De Franceschi, F. Beltram, C. Marinelli, L. Sorba, M. Lazzarino, B.H. Muller, and A. Franciosi, Appl. Phys. Lett. **72**, 1996 (1998).

[6] L. Sorba, S. Yildirim, M. Lazzarino, A. Franciosi, D. Chiola, and F. Beltram, Appl. Phys. Lett. **69**, 1927 (1996); G. Gigli, M. Lomascolo, M. De Vittorio, R. Cingolani, A. Cola, F. Quaranta, L. Sorba, B. Mueller, and A. Franciosi, *ibid.* **73**, 259 (1998).

[7] T. dell'Orto, J. Almeida, A. Terrasi, M. Marsi, C. Coluzza, G. Margaritondo, and P. Perfetti, Phys. Rev. B **50**, 18 189 (1994); J. Almeida, C. Coluzza, T. dell'Orto, G. Margaritondo, A. Terrasi, and J. Ivanco, J. Appl. Phys. **81**, 292 (1997).

[8] M. Cantile, L. Sorba, S. Yildirim, P. Faraci, G. Biasiol, A. Franciosi, T.J. Miller, and M.I. Nathan, Appl. Phys. Lett. **64**, 988 (1994); M. Cantile, L. Sorba, P. Faraci, S. Yildirim, G. Biasiol, G. Bratina, A. Franciosi, T.J. Miller, M.I. Nathan, and L. Tapfer, J. Vac. Sci. Technol. B **12**, 2653 (1994).

[9] K. Koyanagi, S. Kasai, and H. Hasegawa, Jpn. J. Appl. Phys., Part 1 **32**, 502 (1993).

[10] J.C. Costa, F. Williamson, T.J. Miller, K. Beyzavi, M.I. Nathan, D.S.L. Mui, S. Strite, and H. Morkoç, Appl. Phys. Lett. **58**, 382 (1991); J.C. Costa, T.J. Miller, F. Williamson, and M.I. Nathan, J. Appl. Phys. **70**, 2173 (1991); T.J. Miller and M.I. Nathan, Appl. Phys. Lett. **61**, 2332 (1992).

[11] M. Lazzarino, G. Scarel, S. Rubini, G. Bratina, L. Sorba, A. Franciosi, C. Berthod, N. Binggeli, and A. Baldereschi, Phys. Rev. B **57**, R9431 (1998).

[12] W. Chen, A. Kahn, P. Soukiassian, P.S. Mangat, J. Gaines, C. Ponzoni, and D. Olego, J. Vac. Sci. Technol. B **12**, 2639 (1994).

[13] See, e.g., A. Barinov, L. Casalis, L. Gregoratti, and M. Kiskinova, Phys. Rev. B **63**, 085308 (2001); S. Picozzi, A. Continenza, G. Satta, S. Massidda, and A.J. Freeman, *ibid.* **61**, 16 736 (2000).

[14] *Electronic Structure of Metal-Semiconductor Contacts*, edited by

W. Mönch (Jaca, Milano, 1990).
[15] V. Heine, Phys. Rev. **138**, A1689 (1965).
[16] J. Tersoff, Phys. Rev. Lett. **52**, 465 (1984).
[17] F. Flores and C. Tejedor, J. Phys. C **20**, 145 (1987); F. Guinea, J. Sánchez-Dehesa, and F. Flores, *ibid.* **16**, 6499 (1983).
[18] W. Spicer, Semicond. Semimetals **38**, 449 (1993).
[19] J.M. Woodall and J.L. Freeouf, J. Vac. Sci. Technol. **21**, 574 (1982).
[20] G. Margaritondo and P. Perfetti, in *Heterojunction band discontinuities*, edited by F. Capasso and G. Margaritondo (North-Holland, Amsterdam, 1987), p. 59.
[21] S.G. Louie, J.R. Chelikowsky, and M.L. Cohen, Phys. Rev. B **15**, 2154 (1977).
[22] J.P. Sullivan, R.T. Tung, D.J. Eaglesham, F. Schrey, and W.R. Graham, J. Vac. Sci. Technol. B **11**, 1564 (1993).
[23] S.B. Zhang, M.L. Cohen, and S.G. Louie, Phys. Rev. B **32**, 3955 (1985).
[24] R.G. Dandrea and C.B. Duke, J. Vac. Sci. Technol. B **11**, 1553 (1993).
[25] R.J. Needs, J.P.A. Charlesworth, and R. Godby, Europhys. Lett. **25**, 31 (1994); J.P.A. Charlesworth, R. Godby, R.J. Needs, and L.J. Sham, Mater. Sci. Eng., B **B14**, 262 (1992).
[26] C. Berthod, N. Binggeli, and A. Baldereschi, Europhys. Lett. **36**, 67 (1996); C. Berthod, J. Bardi, N. Binggeli, and A. Baldereschi, J. Vac. Sci. Technol. B **14**, 3000 (1996).
[27] A. Ruini, R. Resta, and S. Baroni, Phys. Rev. B **56**, 14 921 (1997).
[28] J. Bardi, N. Binggeli, and A. Baldereschi, Phys. Rev. B **59**, 8054 (1999).
[29] W.E. Pickett, Comput. Phys. Rep. **9**, 117 (1989).
[30] N. Troullier and J.L. Martins, Phys. Rev. B **43**, 1993 (1991).
[31] The Ga $3d$ and Zn $3d$ electrons were treated as frozen core orbitals. It has been shown that including the Ga $3d$ orbitals in the valence shell amounts to including a rigid (semiconductor bulk-like) correction of -0.1 eV on the Al/GaAs SBH, which we neglect here.
[32] L. Kleinman and D.M. Bylander, Phys. Rev. Lett. **48**, 1425 (1982).
[33] D.M. Ceperley and B.J. Alder, Phys. Rev. Lett. **45**, 566 (1980).
[34] H.J. Monkhorst and J.D. Pack, Phys. Rev. B **13**, 5188 (1976).
[35] C. Berthod, N. Binggeli, and A. Baldereschi, Phys. Rev. B **57**, 9757 (1998).
[36] C. Berthod, N. Binggeli, and A. Baldereschi (unpublished).
[37] R. M. Dreizler and E. K. U. Gross, *Density Functional Theory* (Springer-Verlag, Berlin, 1990).
[38] C.J. Fall, N. Binggeli, and A. Baldereschi, Phys. Rev. B **58**, R7544 (1998).
[39] X. Zhu and S.G. Louie, Phys. Rev. B **43**, 14 142 (1991).
[40] The GW calculations for Ge and AlAs in Ref. 39 have been performed using the von Barth-Hedin form of the exchange-correlation potential. The quasiparticle correction to the LDA band gap is more or less independent of the choice of the exchange-correlation potential, but the distribution of this correction between the valence and conduction bands depends on this choice [X. Blase (private communication)]. Since we employ the Ceperley-Alder exchange potential in our calculations, we prefer to use the correction of Ref. 25 for GaAs, based on this potential, and only the difference between the Ge, AlAs, and GaAs corrections of Ref. 39.
[41] O. Zakharov, A. Rubio, X. Blase, M.L. Cohen, and S.G. Louie, Phys. Rev. B **50**, 10 780 (1994).
[42] Landolt-Börnstein, *Numerical Data and Functional Relationships in Science and Technology* (Springer, New York, 1982).
[43] In Ref. 35, the many-body and spin-orbit correction used for the Al/GaAs SBH was 0.21 eV, and not 0.11 eV as indicated by mistake in the caption of Table I.
[44] L.J. Brillson, I.M. Vitomirov, A. Raisanen, S. Chang, R.E. Viturro, P.D. Kirchner, G.D. Pettit, and J.M. Woodall, Appl. Surf. Sci. **65**, 667 (1993).
[45] A. Thanailakis and D.C. Northrop, Solid-State Electron. **16**, 1383 (1973).
[46] S. M. Sze, *Physics of Semiconductor Devices* (Wiley, New York, 1981).
[47] N.M. Johnson, T.J. Magee, and J. Peng, J. Vac. Sci. Technol. **13**, 838 (1976).
[48] A.Y. Cho and P.D. Dernier, J. Appl. Phys. **49**, 3328 (1978).
[49] W.I. Wang, J. Vac. Sci. Technol. B **1**, 574 (1983).
[50] C. Barret and J. Massies, J. Vac. Sci. Technol. B **1**, 819 (1983).
[51] S.J. Eglash, M.D. Williams, P.H. Mahowald, N. Newman, I. Lindau, and W.E. Spicer, J. Vac. Sci. Technol. B **2**, 481 (1984).
[52] J.R. Waldrop, Appl. Phys. Lett. **47**, 1301 (1985).
[53] M. Missous, E.H. Rhoderick, and K.E. Singer, J. Appl. Phys. **60**, 2439 (1986).
[54] S.J. Eglash, N. Newman, S. Pan, D. Mo, K. Shenai, W.E. Spicer, F.A. Ponce, and D.M. Collins, J. Appl. Phys. **61**, 5159 (1987).
[55] M. Missous, W.S. Truscott, and K.E. Singer, J. Appl. Phys. **68**, 2239 (1990).
[56] A. Bosacchi, S. Franchi, E. Gombia, R. Mosca, F. Fantini, R. Menozzi, and S. Naccarella, Electron. Lett. **30**, 820 (1994).
[57] M. Vos, F. Xu, Steven G. Anderson, J.H. Weaver, and H. Cheng, Phys. Rev. B **39**, 10 744 (1989).
[58] Al can be classified as a reactive metal [see, e.g., C.I. Wu, A. Kahn, A.E. Wickenden, D. Koleske, and R.L. Henry, J. Appl. Phys. **89**, 425 (2001)]. In the case of Al/GaAs (100), in particular, a Ga-Al exchange reaction yielding excess GaAlAs at the interface is known to take place [S.A. Chambers, Phys. Rev. B **39**, 12 664 (1989)]. It should be noted, however, that if the transitivity rule holds at the Al/GaAs, Al/GaAlAs, and GaAs/GaAlAs interfaces (see Ref. 28 for a discussion), the presence of a GaAlAs interlayer should have no effect on the Al/GaAs Schottky barrier.
[59] S. Baroni, R. Resta, A. Baldereschi, and M. Peressi, in *Proceedings of NATO Advanced Research Workshop on Spectroscopy of Semiconductor Microstructures*, edited by G. Fasol *et al.* (Plenum, New York, 1989), p. 251; A. Baldereschi, M. Peressi, S. Baroni, and R. Resta, in *Semiconductor Superlattices and Interfaces*, Proceedings of the International School of Physics "Enrico Fermi," Course CXVII, Varenna, 1991, edited by L. Miglio and A. Stella (Academic, New York, 1993), p. 59.
[60] M. Peressi, N. Binggeli, and A. Baldereschi, J. Phys. D **31**, 1273 (1998).
[61] A. Franciosi and C.G. Van de Walle, Surf. Sci. Rep. **25**, 1 (1996).
[62] It should be noted that $\Delta n_a(\boldsymbol{r})$ $[\Delta n_c(\boldsymbol{r})]$ in Eq. (3) is neutral, and carries no dipole nor quadrupole [except for the second spherical moment of the charge given by Eq. (3)], because of the tetrahedral T_d symmetry of the impurity site (see Ref. 59 or 60). The integral in Eq. (3) is therefore well defined; in particular, the result does not depend on the choice of the origin.

[63] A.M. Cowley and S.M. Sze, J. Appl. Phys. **36**, 3212 (1965).

[64] Justification for the general use of an exponential decay of the MIGS can be found, e.g., in A. Ruini, Ph.D thesis, SISSA, 1997, http://www.sissa.it/cm/phd.php; see, e.g., Figs. 7.1 and 7.10 therein.

[65] We note that a somewhat larger value of δ_s (3.2 Å) was used in Ref. 26 to model the effect of Si interlayers on the Al/GaAs SBH. In the latter study, δ_s was not calculated from first principles, but taken as a parameter value giving good general agreement with the SBH modifications induced in a junction containing up to two Si monolayers. The estimated uncertainty on the present δ_s calculated for the unperturbed Al/X junction is about ± 0.2 Å. This uncertainty takes into account deviations of $N(E_{\mathrm{F}}, x)$ from an ideal exponential function, which give rise to some variations of δ_s with x. Such a change in δ_s, however, has a small influence on the model results in Fig. 6(c) and Table II (12% at most).

[66] The theoretical macroscopic dielectric constants, ϵ_∞, have been calculated using the capacitor model of M. Peressi *et al.*, Phys. Rev. B **43**, 7347 (1991). We find $\epsilon_\infty^{\mathrm{GaAs}} = 12.4$, $\epsilon_\infty^{\mathrm{AlAs}} = 9.1$, and $\epsilon_\infty^{\mathrm{ZnSe}} = 6.2$; the experimental values are 10.9, 8.2, and 6.3 for GaAs, AlAs, and ZnSe, respectively.

[67] Using $x_0 = 0.5$ Å in the model, Eq. (11), yields $\Delta\phi_p^{\mathrm{mod}} = 0.14$, 0.17, and 0.55 eV for GaAs, AlAs, and ZnSe, respectively. Scaling, instead, the x_0 value obtained for GaAs (0.6 Å) with the ratio $\delta_s^X/\delta_s^{\mathrm{GaAs}}$, the corresponding results are 0.10, 0.18, and 0.65 eV, respectively. In both cases, the model results give satisfactory agreement with the values calculated *ab initio*.